UNIVERSITY OF CALIFORNIA SAN DIEGO

Promoters for Targeted Gene Delivery to Cortical or Spinal Motor Neurons

A thesis submitted in partial satisfaction of the requirements for the degree Master of Science

in

Biology

by

Bryan Chavez

Committee in charge:

Professor Mark Tuszynski, Chair

Professor Stacey Glasgow, Co-Chair

Professor Yimin Zou

2021

The thesis of Bryan Chavez is approved, and it is acceptable in quality and form for publication on microfilm and electronically.

University of California San Diego

2021

EPIGRAPH

“My life is all I have

My rhymes, my pen, my pad

And I done made it out the struggle, don't judge me

What you sayin' now won't budge me

'Cause where I come from…so often…

People you grow up with layin' in a coffin

But I done made it through the pain and strife

It's my time now, my world, my life, my life.”

Excerpt from “my . life”
Written by Jermaine Lamarr Cole, Shéyaa Bin Abraham-Joseph, and Morae Ruffin

TABLE OF CONTENTS

LIST OF FIGURES

ACKNOWLEDGEMENTS

I would like to thank Dr. Mark H. Tuszynski for allowing me to work in his lab and for providing me with the space to grow as a scientist. I would also like to thank Lori Graham for giving me the chance to work and be promoted within the lab.

I would also like to thank Dr. Michael J. Castle for designing a stimulating project that fit my goals as a student, and for taking the time to teach me the skills necessary to complete the project. I have learned a lot of critical skills that I will surely continue to use in my career inside and outside of the lab.

I would also like to thank my co-chair, Professor Stacey Glasgow, and my thesis committee member Professor Yimin Zou for their feedback and support.

Finally, I would like to thank my girlfriend, family, and friends for their continuous love and support.

ABSTRACT OF THE THESIS

Promoters for Targeted Gene Delivery to Cortical or Spinal Motor Neurons

by

Bryan Chavez

Master of Science in Biology

University of California San Diego, 2021

Professor Mark Tuszynski, Chair

Professor Stacey Glasgow, Co-Chair

Adeno-associated viral (AAV) vectors are effective gene therapy delivery candidates, and the AAV-PhP.eB capsid is effective at transducing the CNS in mice when delivered intravenously (IV). Introduction of promoter sequences to the AAV-PhP.eB genome can restrict gene expression to specific cell types. More research is needed to identify cell-specific promoter sequences that restrict gene expression to specific CNS targets. Thus, the Ple394 and Ple394-HBB sequences were examined to see if they can restrict gene expression to cortical neurons. The HB9 sequence was examined to see it could restrict gene expression to spinal motor neurons. The Ple394 promoter resulted in strong cortical neuron gene expression and comparatively less gene expression in off-target brain and spinal cord regions. The Ple394 vector did not result in significantly different gene expression in the liver compared to mice that

received saline. The Ple394-HBB promoter failed to cause cortical neuron-specific gene expression. The HB9 promoter resulted in spinal motor neuron-specific gene expression with relatively little expression in the brain. The HB9 vector didn't result in significantly different gene expression in the liver compared to mice that received saline. In conclusion, introduction of the Ple394 and HB9 promoter sequences into the AAV-PhP.eB genome were able to restrict gene expression to cortical neurons and spinal motor neurons, respectively. Identification of promoters that can drive selective gene expression in the cerebral cortex or spinal motor neurons will allow for the IV delivery of AAV gene therapies to treat diseases such as Alzheimer's disease or amyotrophic lateral sclerosis, respectively.

Introduction

Gene Therapy

Gene therapy research has grown in popularity to treat a variety of diseases, because it offers a platform to treat illnesses with the use of a single administration of medication, compared to the multiple doses required for typical protein-based pharmaceuticals (Dunbar et al., 2018). Gene therapy is the use of some form of viral or non-viral vehicle to deliver nucleic acids to patient cell's genome, and then allowing the cells to utilize their own machinery to transcribe and translate the delivered genetic material into the protein product (Dunbar et al., 2018). The protein product could range in identity, depending on the disease one is attempting to cure. There are currently a handful of gene therapy-based medications available for human use based on data from the Food & Drug Administration (FDA) (US Food & Drug Administration, 2021). Despite this, there are limitations to the widespread use of gene therapy to cure disease including potential toxicity from off-target genome editing, and the need to identify the most efficient delivery vehicles (Dunbar et al., 2018).

Adeno-Associated Viruses in Gene Therapy

Adeno-associated virus (AAV) vectors have been shown to be effective gene therapy delivery candidates based on their safety and ability to sustain gene expression over extended time periods (Wang et al., 2019). The AAV, which originates from human parvovirus, is known to not be pathogenic and does not cause disease in humans (Hermonat et al., 1984). This virus contains a single-stranded DNA genome that is about 4.7 kilobases long, and this genome can be edited at specific regions to include the genetic sequence of the protein one desires to be expressed in the receiving host (Wang et al., 2019). The AAV vector, upon administration into a

subject, undergoes specific interactions between its capsid and the host cell's surface receptors, which lead to the virus entering the cell (Schultz et al., 2008). After internalization, downstream reactions eventually lead to the expression of the desired gene, or transgene.

A potential drawback of the use of AAV is that their genome is relatively small, only about 5 kb as previously mentioned, which limits the size of the gene one would like to deliver (Dunbar et al., 2018). In addition, this virus is replication-defective meaning that it cannot be used to target dividing cells since the virus will not be able to replicate itself and exert its effects on other cells (Dunbar et al., 2018). Despite the drawbacks, the AAV vector model is a favorable candidate to deliver genetic material that is below its size threshold to non-dividing cells, which still allows for potential at curing many diseases. In addition, it's replication deficiency can be seen as a positive feature, because it means that the virus will not spread further than intended (Dunbar et al., 2018).

The targeting of the expression of the gene product toward specific cell or tissue types can be modified through many methods. First, many natural and synthetic variants of AAV have been described, which each have different capsids (Gao et al., 2004). The capsids can be altered to improve cell-specific targeting (Castle et al., 2016). Many capsids are currently known that target a variety of organ systems (Wang et al., 2019). For example, AAV8 is favored for targeting the liver, while AAV2 and AAV9 are favored for targeting the CNS (Wang et al., 2019). Second, the method of vector delivery can also affect the targeting of the therapeutic. Many methods exist for delivery of the vector including direct injections into the organ of interest or intravenous injections (Castle, et al., 2016).

AAV Vectors Used to Treat Neurological Diseases

Kaplitt and colleagues showed that AAV vectors could be used to transduce, introduce foreign DNA, safely and adequately into the rat central nervous system (CNS) (Kaplitt et al., 1994). Interest into being able to effectively transduce the CNS is high since there are many neurological diseases that have no long-term effective treatments or methods to fully cure the disease rather than the symptoms. Neurological diseases of this nature include Alzheimer's disease (AD) and amyotrophic lateral sclerosis (ALS) (Yiannopoulou et al., 2012; Petrov et al., 2017).

AD is a neurodegenerative disorder that results in disruption of memory and eventual loss of other mental functions (Hippius et al., 2003). This disorder has no long-term effective treatments currently approved by the FDA, however there are various gene therapy target candidates being researched. One of these targets is the apolipoprotein (APOE) gene, which is known to play a role in the clearance of amyloid-beta peptides (Verghese et al., 2013). The accumulation of misfolded amyloid-beta peptides is thought to be one of the leading causes of this disease (Serrrano-Pozo et al., 2011). These misfolded amyloid-beta peptides accumulate in the extracellular space in the brain and form plaques that lead to neuronal damage (Serrrano-Pozo et al., 2011). Specifically, the E4 allele of the APOE gene is known to be a risk factor for the development of late-onset AD, due to lack of amyloid-beta plaque clearance seen in those with this allele (Sanders et al., 1993). The E2 allele, on the other hand, is thought to be protective against development of AD (Farrer et al., 1997). Therefore, AAV gene therapy research has focused on expressing the APOE E2 allele in the CNS of subjects who are affected by the APOE E4 allele, and this research has shown that the introduction of the APOE E2 allele can decrease the amount of amyloid-beta plaque present in the CNS of mice (Zhao et al., 2016). In addition, AAV vectors have been studied to treat ALS, which is a neurodegenerative disease where motor

neurons are lost and can eventually lead to the fatal loss of muscle and strength (Rowland, 2001). The increased interest in using the AAV as a model to treat neurological disorders thus warrants further investigation into the identification of vector serotypes, or variants, and infusion methods that improve cell targeting and on-target gene expression.

As previously mentioned, the AAV vectors also come in a variety of serotypes. The AAV2 capsid has historically been one of the most widely used vectors for gene therapy delivery into the CNS (Manfredsson et al., 2009; Chan et al., 2017). This vector had to be delivered directly into the targeted brain region to produce an effect, because of their inability to cross the blood brain barrier (BBB) (Manfredsson et al., 2009; Chan et al., 2017). These delivery methods, however, are invasive since they involve brain surgery. Also, to achieve widespread distribution of the vector, which would be desired if one was attempting to treat a disease that affects a large area of the CNS, then one may have to perform multiple direct brain injections (Chan et al., 2017). These drawbacks and inability to guarantee a widespread distribution of the treatment may falsely lead to one seeing no effect if treatment is delivered to treat a certain disease. Castle and colleagues elaborate that this may have been what occurred in an AD trial using AAV2 to deliver nerve growth factor to the brain to promote neuronal survival (Castle et al., 2020). Another commonly used vector for neurological delivery, AAV9, does have the ability to cross the BBB in rodents and non-human primates, which offers a potential method of delivering gene therapies to the CNS intravenously (Manfredsson, 2009). However, when the AAV9 vector is delivered intravenously, it lacks the ability to transduce specific areas of the CNS and instead targets a variety of CNS areas and even other tissues such as the heart, liver, and kidneys (Mori et al., 2006). This may lead to off-target gene expression, which may lead to toxicity (Mori et al., 2006). In addition, intravenous delivery of AAV9 results in lower gene expression in neurons

targeted, which means that the dose of AAV9 needed would have to be higher to produce a notable effect. This may lead to increases in production costs (Foust & Kasper, 2009).

In response to the need for more effective vectors, work was done to identify the most effective AAV capsids for transducing a desired target cell type (Deverman et al., 2016; Chan et al., 2017). Recent work by Chan et al. shows that the AAV-PhP.eB capsid is effective at transducing the CNS in mice when delivered intravenously at lower doses than previously used vectors. The mechanism by which this vector crosses the BBB has also been studied, and it has been found that it does so by interacting with the LY6A receptor (Huang et al., 2019). Research on this capsid has showed that when delivered intravenously, the PhP.eB variant was better at transducing cells in the CNS than its parent variants, AAV9 and AAV-PhP.B even at lower doses (Chan et al., 2017; Kumar et al., 2020). In addition, research has also shown that the AAV-PhP.eB capsid produces lower gene expression in the liver compared to AAV9 after IV injection (Mathiesen et al., 2020). The selectivity and effectiveness of the PhP.eB variant means that one would need lower doses and leads to reduced risk of off-target side effects. However, this variant has not been shown to be safe or effective in humans yet.

In addition to identifying new capsids for better gene delivery, the vector genome can also be edited for these purposes. Within the vector genome, there is a promoter sequence region (Naso et al., 2017). This region is necessary for gene expression to occur from the gene delivered by the vector (Naso et al., 2017). The promoter is a sequence of DNA that initiates transcription of the gene of interest (Naso et al., 2017). It is common to use a general non-cell-specific promoter such as the CAG promoter in vector constructs (Naso et al., 2017). The CAG sequence contains the 380 bp cytomegalovirus enhancer region, the 278 bp chicken β-actin promoter, and the first exon (90 bp) and first intron (922 bp) of the chicken β-actin gene (Figure 1). The CAG

promoter sequence is known to be strong and general, allowing many cell types to begin transcription when it is present in the delivered sequence (Niwa et al., 1991). Thus, the CAG promoter has historically been used in vector constructs resulting in a high amount of expression of the desired gene product (Naso et al., 2017). With the discovery of vectors that can be intravenously injected and thus delivered to a wide range of organ systems at once, it is important to begin thinking about the restriction of the organ systems that are expressing the gene product delivered. Certain gene products are favored to be expressed in the cell types one is targeting, but the same products may cause negative effects elsewhere in the body. This is known as off-target toxicity (Dunbar et al., 2018). Thus, research into cell-specific promoters, which can replace the CAG promoter sequence in the vector sequence, can enhance the targeting of the transduction, and improve the expression of gene product in desired cell types (Chan et al., 2017).

Discovering Promoter Sequences to Target Specific Neuronal Cell Types

The identification of cell-specific promoters, which when added to the vector sequence, can lead to a future of sophisticated vector libraries that contain various vectors to choose from depending on the cell or tissue target. For example, if there was interest in treating AD, one may desire to use a vector that can specifically target the cerebral cortex, one of the main brain areas affected by the disease (Fjell et al., 2014). A potential cerebral cortex specific promoter is the novel 2,232 kb Ple394 sequence. This promoter sequence derives its name from the Pleiades Promoter Project, which has developed an array of promoters as tools to enhance the study of gene therapies and targeted gene expression (Portales-Casamar et al., 2010; Leeuw et al., 2014). Research by Porateles-Casamar and colleagues (2010) identified the 2,603 bp Ple17 promoter sequence and showed that this sequence effectively restricted gene expression to the cortex using

AAV as the delivery method. The original Ple17 promoter sequence, however, contains extraneous sequence that is left over from the reactions necessary to identify promoter sequence candidates (Portales-Casamar et al., 2010; Leeuw et al., 2014). Thus, removal of these "junk" sequences led to the construction of the novel 2,232 bp Ple394 promoter sequence, a sequence that has not yet been studied. The interest in the Ple394 sequence over the Ple17 sequence revolves around the fact that the AAV vector has limited space in its genome, and thus saving space can lead to more available space for the therapeutic gene one wants to deliver. Comparisons of the size difference between these promoter constructs are shown in Figure 1. Moreover, if one desired to treat ALS, which mainly affects motor neurons, then one would desire a vector that specifically targets these cell types. A potential spinal motor neuron specific promoter is the HB9 promoter. This promoter has been described to be selectively expressed in spinal motor neurons (Arber et al., 1999; Peviani et al., 2011; Nakano et al., 2005; Lee et al., 2004). The original identification of the 9 kb sequence of the HB9 promoter was reported by Arber and colleagues (1999). The identification of the 2.5 kb essential portion of the HB9 promoter as well as the M250 enhancer was described by Lee and colleagues (2004). This essential sequence and the M250 enhancer region were used in these experiments. An additional essential 313 base pair enhancer region of the promoter was identified by Nakano and colleagues (2005). This region was also included in the sequence used in these experiments. Research has also been performed using an essential 1.6 kb long fragment of the HB9 promoter with lentivirus, which showed promise in targeting spinal motor neurons in mice (Peviani et al., 2012). The entire sequence used in those experiments consisted of a 3,610 bp HB9 promoter sequence (Figure 1). The HB9 sequence used in these experiments consists of this 1.6 kb essential region and the M250 enhancer previously mentioned, leading to a 2,405 bp HB9

promoter described in Figure 1. The Ple394 and HB9 sequences, to our knowledge, have not been used in an AAV vector construct, so research that studies the effectiveness of these promoters to restrict gene expression after AAV infusion to cortical neurons and spinal motor neurons respectively, is warranted.

Further research is also warranted on replacing other components of the vector genome. For example, the 68 bp cytomegalovirus (CMV) minimal promoter region, which was present in the HB9 promoter vector construct used in previous studies by Peviani and colleagues (2012) may be the cause of reduced gene expression due to high methylation of this region (Brooks et al., 2004). The reason for this methylation could be due to the viral origins of the CMV promoter region (Brooks et al., 2004). Replacing this CMV sequence with a sequence that is found in nonviral organisms, such as humans, may decrease the methylation that occurs and thus improve gene expression. A potential sequence of interest is the 57 bp human beta-globin (HBB) minimal promoter sequence. The essential sequence of the HBB minimal promoter and its non-canonical transcription start site is described by Leach and colleagues (2003). Further, research in mice has been done showing that using the HBB minimal promoter sequence with different cell-type specific enhancers does not alter the specificity of the enhancers used (Hrvatin et al., 2019). The HBB minimal promoter sequence is thus present in the HB9 vector construct used in these experiments. In addition, an alternate Ple394 vector construct in which the Ple394 core promoter region is replaced with the HBB minimal promoter while still retaining the Ple394 enhancer regions was constructed and studied in these experiments. The rationale behind making the Ple394-HBB vector construct was to replace portions of the large 2,232 Ple394 promoter sequence with the smaller 57 bp HBB sequence, which would free up 656 bp of space within the vector genome for a therapeutic gene sequence to be added for future research (Figure 1). The

AAV capsid is known to have a limited 4.7 kilobase long genome so shortening the promoter sequence would improve upon its capacity to hold larger therapeutics (Wang et al., 2019). An additional component of the vector genome that can be altered is the inclusion of a synthetic intron. Introns are known to cause an increase in gene expression (Shaul, 2017). Thus, research into the use of a synthetic intron (SI), one that is not normally present and was instead added to the vector sequence, is warranted to improve expression of the delivered gene. A 110 bp SI sequence was included in the experimental vectors used in these experiments (Figure 1). This short synthetic intron sequence was first described by Chan, et al. (2017).

My project revolved around the exploration of the AAV-PhP.eB-Ple394-SI (Ple394), AAV-PhP.eB-Ple394-HBB-SI (Ple394-HBB), and AAV-PhP.eB-HB9-HBB-SI (HB9) vector sequences. The HB9 vector construct was made to include the HBB minimal promoter sequence (HB9). Two vector constructs were made using the Ple394 promoter sequence, one where the core promoter sequence remained intact (Ple394) and one where the core promoter sequence was replaced with the minimal HBB sequence (Ple394-HBB). The research questions of this project were: Can introduction of the Ple394 and Ple394-HBB promoter sequences into AAV-PhP.eB capsids effectively restrict gene expression to cortical neurons, and prevent gene expression in other cell types? Can introduction of the HB9 promoter sequence into the AAV-PhP.eB capsid effectively restrict gene expression to spinal motor neurons, and prevent gene expression in other cell types? First, a dose-escalation experiment was conducted to determine the best dose of each vector-promoter construct that causes favorable gene expression in the CNS after intravenous injection of the vector. Three doses were explored based on work done by Chan and colleagues (2017) on the vector construct, PhP.eB. Second, the best dose from the first experiment was used to treat a larger sample of animals to perform an experimental comparison of the experimental

vectors to positive and negative control groups in terms of their off-target gene expression in peripheral organs. We hypothesized that intravenous administration of the Ple394 and Ple394-HBB vector constructs would lead to a minimal in off-target gene expression while maintaining strong gene expression in cortical, and the HB9 vector construct would lead to minimal of off-target transduction while maintaining strong gene expression in spinal motor.

Results

We tested the effect of three promoter sequences on AAV gene expression targeting. The reporter gene enhanced green fluorescent protein (eGFP) was used to visualize cells that were able to express the vector's delivered gene. We tested the sequence, AAV-PhP.eB-Ple394-SI (Ple394), amongst three dosing groups. We also tested an AAV-PhP.eB-Ple394-HBB-SI (Ple394-HBB) sequence in mice that received the same dose as the medium dose group used in the Ple394 experiment delivered intravenously. Finally, we tested the AAV-PhP.eB-HB9-HBB-SI (HB9) sequence amongst three dosing groups. We used the AAV-PhP.eB-CAG sequence as positive control since the CAG sequence is known to be a general non-cell-specific promoter that results in non-specific gene expression of the delivered gene. We used saline as negative control. The vector constructs are outlined in Figure 1.

Ple394

Intravenous injections of the Ple394 vector were given through the retro-orbital sinus to fourteen mice (seven female and seven male). Three dosages of this vector were used: $6.25x10^{10}\ vg/150mL$ (two males and one female), $1.25x10^{11}\ vg/150mL$ (four males and five females), $2.50x10^{11}\ vg/150mL$ (one male and one female). The mice were all treated with 150μL of intravenous AAV-PhP.eB-Ple394 diluted in PBS. The Ple394 construct was constructed to target gene expression to cortical brain regions. To assess the specificity of gene expression targeting by the Ple394 vector, brain sections from the mice were immunostained against eGFP, the cervical spinal cords of the mice were immunostained against eGFP, and quantitative reverse-transcriptase polymerase chain reaction (qRT-PCR) experiments were performed to measure expression of eGFP in the livers of these mice. First, brains were stained

against eGFP and representative lateral and intermediate sections from each dose group are shown in Figure 2. Transduced neurons labeled by antibodies against eGFP present as small, dark-colored cell bodies with axonal and dendritic processes. In figure 2, a red arrow is used to show an example of an eGFP stained neuron. Comparison of the positive control CAG images to the Ple394-treated group images shows that the Ple394 promoter almost eliminated gene expression in non-cortical brain regions such as cerebellum, striatum, and thalamus, while still strongly expressing in cortical regions such as the frontal and entorhinal cortex as shown by the number of eGFP labeled cells in each tissue segment (Figure 2). One off-target area that still showed gene expression was the brainstem, which showed increased expression, as indicated by an increase in the number of eGFP labeled cell bodies, with an increased dose of the vector (Figure 2). To assess whether other CNS regions also expressed the delivered gene, the cervical spinal cords of the mice were transversely sectioned and fluorescent immunostaining against eGFP was performed and the results are shown in Figure 3. The three Ple394-treated groups' images show that the Ple394 vector almost completely lacked off-target gene expression as shown by the absence of eGFP-positive cells in the low dose image, and minimal amount of eGFP-positive cells in the medium and high dose images (Figure 3). Finally, to assess whether peripheral organs also expressed the delivered gene, the livers of the mice were dissected, and qRT-PCR was performed to measure the expression of eGFP in the organ. The results from the qRT-PCR experiments are outlined in Figure 7. The livers of medium dosed-Ple394 mice didn't have significantly different expression of eGFP in the liver compared to mice that received saline (Figure 7). All in all, the introduction of the Ple394 promoter sequence into the AAV-PhP.eB capsid was able to successfully restrict gene expression from off-target CNS regions and other body regions such as the liver, while still leading to strong gene expression in cortical areas.

Ple394-HBB

Intravenous injections of the Ple394-HBB vector were given through the retro-orbital sinus to four mice (two males and two females). The mice received 150µL ($1.25x10^{11}\ vg/150mL$) of intravenous AAV-PhP.eB-Ple394-HBB diluted in PBS. The Ple394-HBB vector was constructed to also target gene expression to cortical brain regions. To assess the specificity of gene expression targeting by the Ple394-HBB vector, brain sections from the mice were immunostained against eGFP. The brains were stained against eGFP and representative lateral and intermediate sections from each mouse from this experiment are shown in Figure 4. Transduced neurons labeled by antibodies against eGFP present as small, dark-colored cell bodies with axonal and dendritic processes. In figure 4, a red arrow is used to show an example of an eGFP stained neuron. Comparison of the intermediate and lateral brain sections from the positive control CAG mouse to the Ple394-HBB group images shows that the Ple394-HBB promoter failed to cause gene expression in cortical brain areas.

All in all, the introduction of the Ple394-HBB promoter sequence into the AAV-PhP.eB capsid was not able to cause gene expression in cortical brain areas.

HB9

Intravenous injections of the HB9 vector were given through the retro-orbital sinus to eighteen mice (eight males and ten females). Three dosages of this vector were used: $6.25x10^{10}\ vg/150mL$ (one males and two females), $1.25x10^{11}\ vg/150mL$ (four males and four females), $2.50x10^{11}\ vg/150mL$ (three males and four females). The mice were all treated with 150µL of intravenous AAV-PhP.eB-HB9-HBB diluted in PBS. The HB9 construct was

constructed to restrict gene expression to spinal motor neurons. To assess the specificity of gene expression targeting by the HB9 vector, cervical spinal cord sections from the mice were immunostained against eGFP, the brains of the mice were immunostained against eGFP, and qRT-PCR experiments were performed to measure expression of eGFP in the livers of these mice. First, the cervical spinal cords were stained against eGFP and representative transverse sections from each dose group are shown in Figure 5. Transduced cells labeled by antibodies against eGFP were confirmed to be motor neurons by colocalization with motor neuron marker, choline acetyltransferase (ChAT). In figure 5, a white arrow is used to show an example of an eGFP stained motor neuron. The three HB9-treated group images show that the HB9 promoter resulted in gene expression almost specifically in motor neurons (Figure 5). The immunostain results suggest that the medium and high dosages resulted in the more gene expression. The high dosage group seemed to have some off-target expression with some eGFP-positive cells being non-motor neurons (Figure 5). To assess whether other CNS regions also expressed the delivered gene, the brains of the mice were sagittally sectioned and immunostaining against eGFP was performed and the results are shown in Figure 6. In figure 6, a red arrow is used to show an example of an eGFP stained neuron. Comparison of the CAG positive control images to the HB9 images shows that the HB9 vector almost eliminated off-target gene expression as shown by the markedly reduced number of eGFP-positive cells in the HB9 treated groups (HB9 low dose, HB9 medium dose, and HB9 high dose). Finally, to assess whether peripheral organs also expressed the delivered gene, the livers of the mice were dissected, and qRT-PCR was performed to measure the expression of eGFP in the organ. The results from the qRT-PCR experiments are outlined in Figure 7. The HB9 vector at the medium and high doses didn’t result in significantly different expression of eGFP in the liver compared to mice that received saline (Figure 7).

All in all, the introduction of the HB9 promoter sequence into the AAV-PhP.eB capsid was able to successfully restrict gene expression from off-target CNS regions and peripheral body regions, while still leading to strong gene expression in spinal motor neurons in the cervical spinal cord.

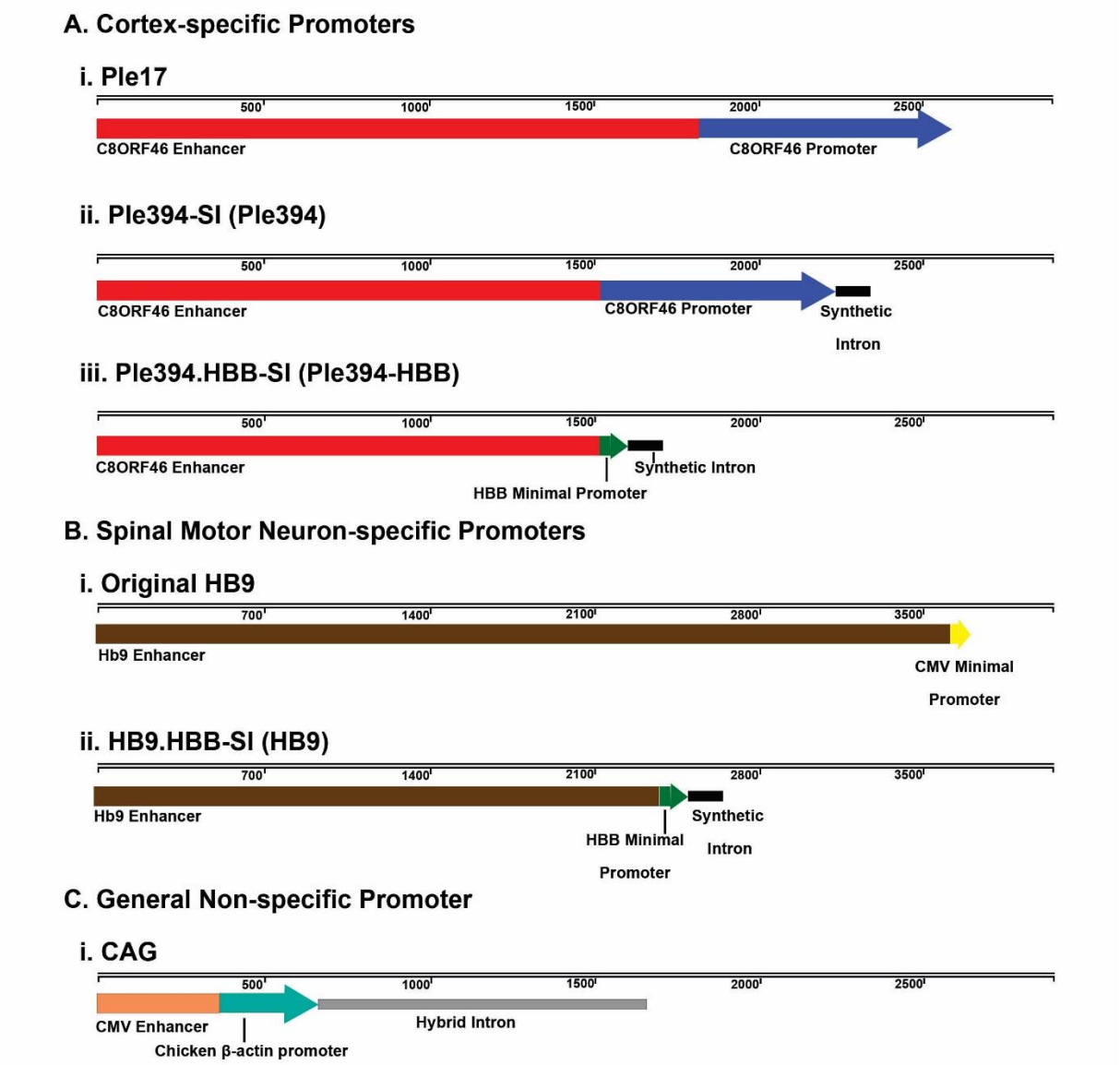

Figure 1. Schematic overview of the vector constructs used in these experiments. A. The cortex-specific promoter constructs used in these experiments. (i) The original 2,603 bp Ple17 sequence identified by Portales-Casamar and colleagues (2010) which features the 1,890 bp C8ORF46 enhancer and 713 bp C8ORF46 promoter. (ii). The 2,232 bp Ple394 sequence used in these experiments, which contains a shortened form of the C8ORF46 enhancer (1,519 bp) and the same C7ORF46 promoter as the Ple17 construct. This construct also contains a 110 bp synthetic intron sequence. (iii). The modified Ple394 sequence which has the same C8ORF46 enhancer as the Ple394 sequence but had the C7ORF46 promoter sequence replaced by the 57 bp HBB sequence. B. The spinal motor neuron-specific promoter constructs used in these experiments. (i). The original 3,610 bp HB9 sequence used by Peviani and colleagues (2012) which features the 68 bp CMV minimal promoter. (ii). The 2,405 bp HB9 sequence used in these experiments, which contains a shortened version of the HB9 sequence shown in (i) and a 110 bp synthetic intron sequence. C. The general non-specific promoter used in these experiments as a positive control vector. (i). The CAG promoter sequence which contains the 380 bp CMV enhancer region, 278 bp chicken β-actin promoter, and a 1,012 bp hybrid intron of the chicken β-actin gene.

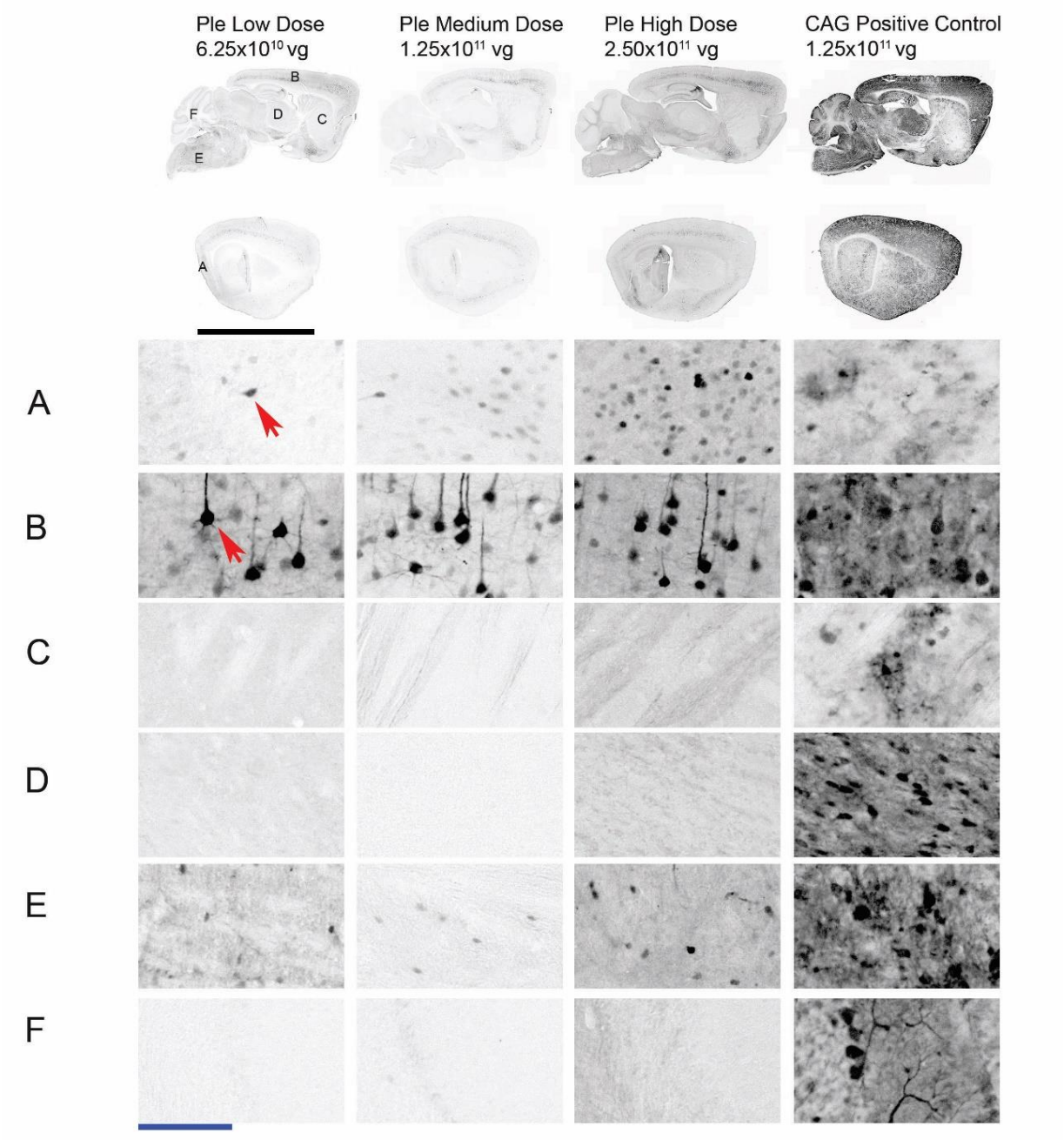

Figure 2. The Ple394 vector sequence results in cortex-specific gene expression after IV injection of AAV-PhP.eB. An immunostain against eGFP was done on 40µm thick sagittal brain sections from mice that received intravenous injections of either AAV-PhP.eB-CAG-eGFP (CAG-Positive Control) or AAV-PhP.eB-Ple394-eGFP at low (Ple394-Low Dose), medium (Ple394-Medium Dose), or high dosages (Ple394-High Dose). A representative intermediate and lateral section of one mouse from each experimental group and positive control group was used to generate the images. From the representative sections, high magnification images of the entorhinal cortex (A), frontal cortex (B), striatum (C), thalamus (D), brainstem (E), and cerebellum (F) were obtained. The lateral sections are roughly 3.25 mm from the midline. The intermediate sections are roughly 1.25 mm from the midline. The entorhinal and frontal cortex are on-target areas. Striatum, thalamus, brainstem, and cerebellum are off-target areas. The red arrow indicates an eGFP stained neuron. Black scale bar: 5,000 µm. Blue scale bar: 100 µm. Red arrow: eGFP-stained neuron.

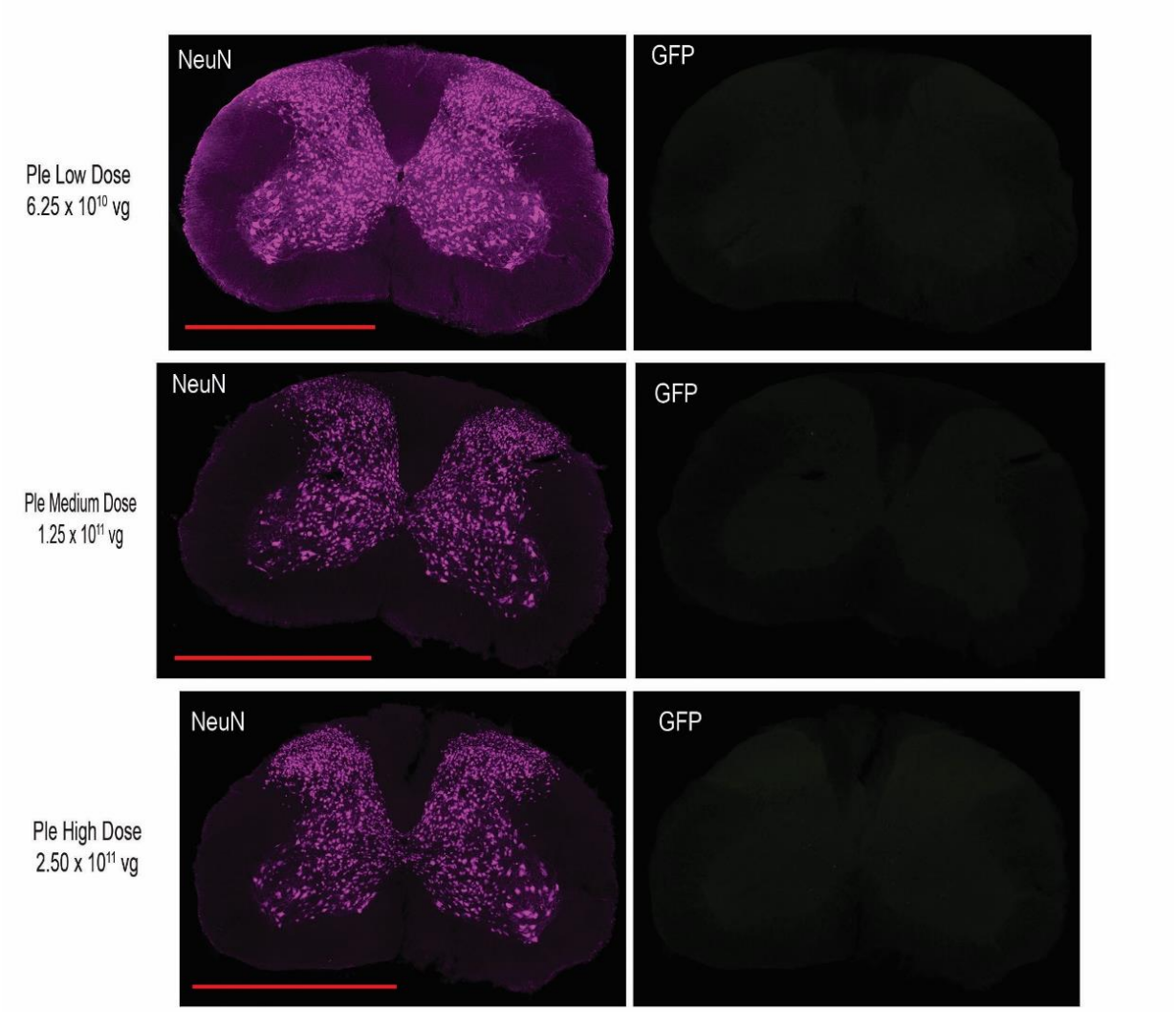

Figure 3. The Ple394 vector sequence restricts gene expression from the cervical spinal cord after IV injection of AAV-PhP.eB. A fluorescent immunostain against viral transgene eGFP (green) and neuron marker, NeuN (violet), was performed on 40 μm thick transverse cervical spinal cord sections from mice that received intravenous injections of AAV-PhP.eB-Ple394 -eGFP at low (Ple Low Dose), medium (Ple Medium Dose), or high dosages (Ple High Dose). Dosages are outlined below the label for each treatment group. One section from a representative mouse is shown for each group. Red scale bars: 500 μm.

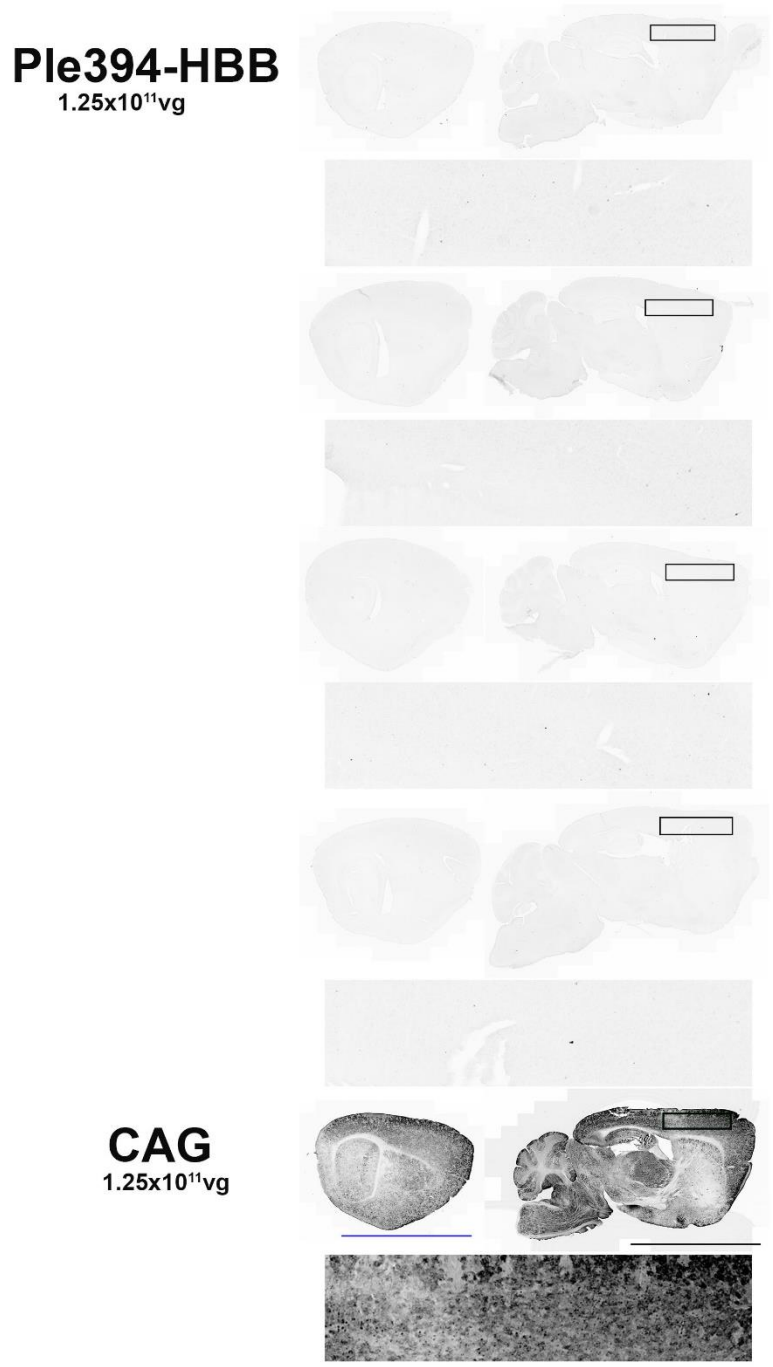

\

Figure 4. The Ple394-HBB vector sequence failed to produce cortex-specific gene expression after IV injection of AAV-PhP.eB. An immunostain against eGFP was done on 40μm thick sagittal brain sections from mice that received intravenous injections of either AAV-PhP.eB-CAG-eGFP (CAG-Positive Control) or AAV-PhP.eB-Ple394-HBB-eGFP (Ple394-HBB). Both vectors were delivered at a dose of $1.25x10^{11}$ vg/150μL. A representative lateral and intermediate section of each mouse (n=4) from the Ple394-HBB experimental group is shown. A representative lateral and intermediate section from one mouse that received the positive control CAG vector is also shown. From the representative sections, high magnification images of the frontal cortex are shown. The lateral brain sections are roughly 3.25 mm from the midline. The intermediate brain sections are roughly 1.25 mm from the midline. Scale bars: 5,000μm.

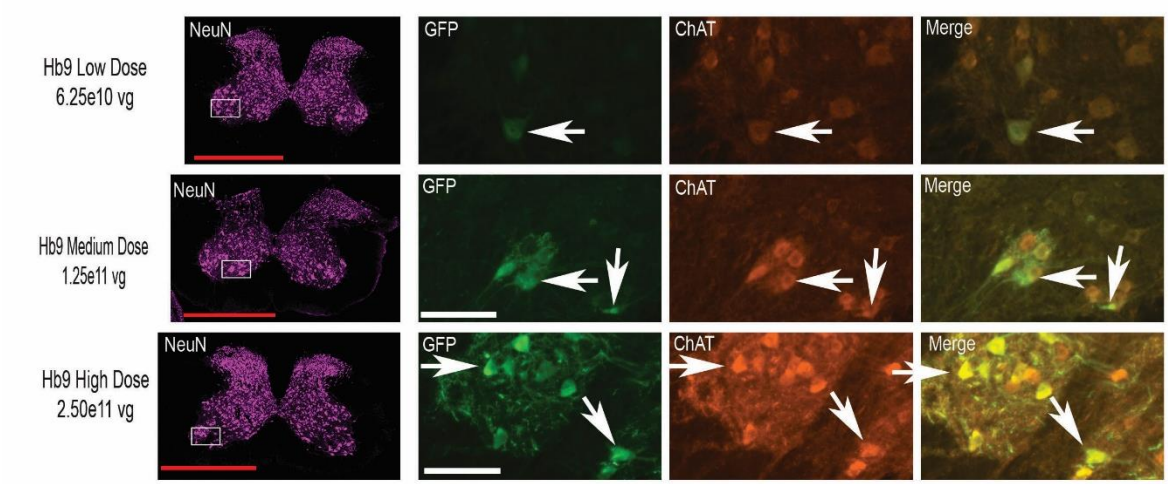

Figure 5. The HB9 vector sequence results in spinal motor neuron-specific gene expression after IV injection of AAV-PhP.eB. A fluorescent immunostain against viral transgene eGFP (green) and motor-neuron marker, ChAT (red), was performed on 40 µm thick transverse cervical spinal cord sections from mice that received intravenous injections of AAV-PhP.eB-Hb9-Hbb-eGFP at low (Hb9 Low Dose), medium (Hb9 Medium Dose), or high dosages (Hb9 High Dose). Dosages are outlined below the label for each treatment group. One section from a representative mouse is shown for each group. Colocalization between eGFP signal and ChAT signal confirmed that the eGFP positive neurons are motor neurons (white arrows). High magnification images of the ventral horn are shown. Red scale bars: 500 µm. White scale bars: 100 µm.

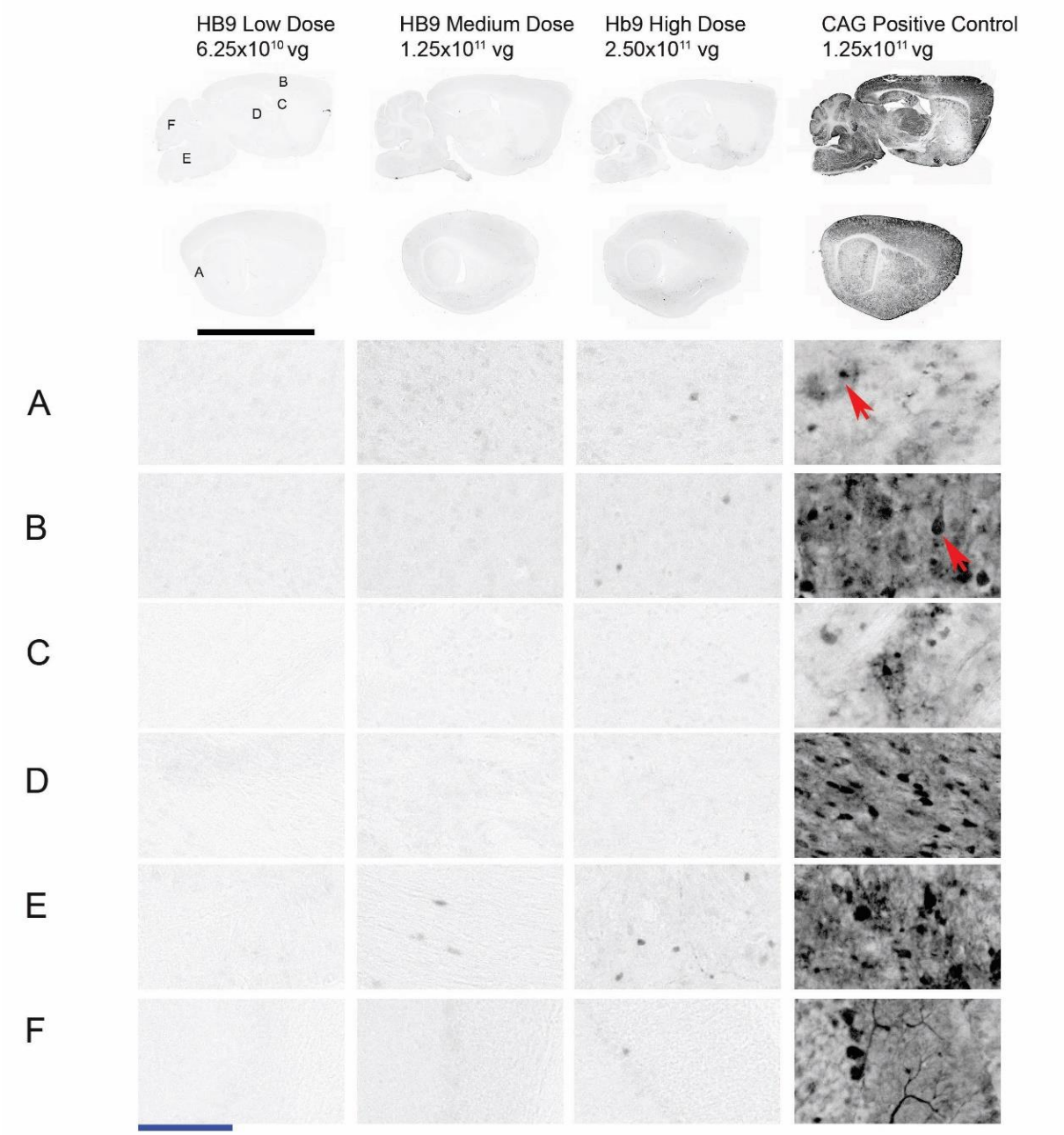

Figure 6. The HB9 vector sequence results in reduced gene expression in the brain after IV injection of AAV-PhP.eB. An immunostain against eGFP was done on 40μm thick sagittal brain sections from mice that received intravenous injections of either AAV-PhP.eB-CAG-eGFP (CAG-Positive Control) or AAV-PhP.eB-HB9-HBB-eGFP at low (HB9-Low Dose), medium (HB9-Medium Dose), or high dosages (HB9-High Dose). A representative intermediate and lateral section of one mouse from each experimental group and positive control group was used to generate the images. From the representative sections, high magnification images of the entorhinal cortex (A), frontal cortex (B), striatum (C), thalamus (D), brainstem (E), and cerebellum (F) were obtained. The lateral sections are roughly 3.25 mm from the midline. The intermediate sections are roughly 1.25 mm from the midline. The entorhinal cortex, frontal cortex, striatum, thalamus, brainstem, and cerebellum are all off-target areas. The red arrow indicates an eGFP stained neuron. Black scale bar: 2,000 μm. Blue scale bar: 100 μm. Red arrow: eGFP-stained neuron.

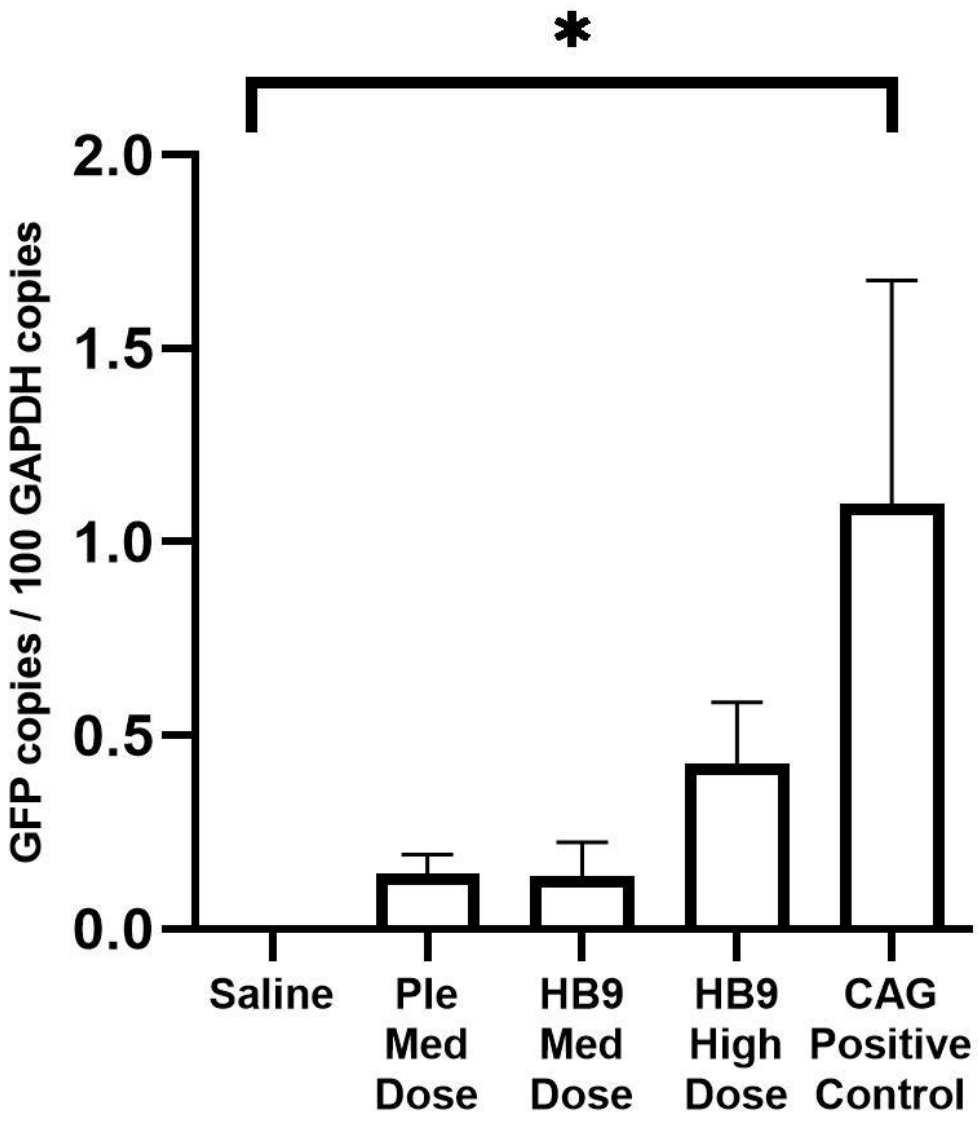

Figure 7. Gene expression in the livers of Ple394 and HB9 treated mice do not significantly differ from saline treated mice. Quantitative reverse transcription-polymerase chain reaction (qRT-PCR) analyses showing housekeeping protein, GAPDH, and viral protein, GFP, mRNA levels were performed on samples of liver from mice that received intravenous injections of either saline, AAV-PhP.eB-CAG-eGFP (CAG Positive Control), AAV-PhP.eB-Ple394-eGFP at medium dose (Ple394 Med Dose), or AAV-PhP.eB-HB9-HBB-eGFP at medium dose (HB9 Med Dose) or high dose (HB9 High Dose). Quantification of the qRT-PCR analyses showing GFP mRNA levels in liver as copies of GFP per 100 copies of GAPDH are summarized from the five groups of mice (mean ± SE; *: significantly different from saline group, $P < 0.05$, One-way ANOVA with Tukey's post-hoc test)

Discussion

Ple394:

The Ple394 vector construct resulted in reduced gene expression of the eGFP reporter gene in off-target brain regions such as the thalamus, cerebellum, and striatum compared to the positive control vector after intravenous (IV) injection (Figure 2). The Ple394 vector construct retained strong expression in cortical areas such as the frontal and entorhinal cortex with some off-target expression in regions such as the brainstem (Figure 2). Additionally, cervical spinal cord immunostain results from mice that received the Ple394 vector show reduced gene expression in this region (Figure 3). In addition, the Ple394 vector at the medium dose didn't result in significantly different expression of eGFP in the liver compared to mice that received saline (Figure 7). Meanwhile, the positive control CAG vector resulted in significantly increased expression of eGFP in the liver compared to saline (Figure 7). It should be noted that some mice in the CAG vector group showed weak eGFP expression in the liver. Past research has shown that the PhP.eB vector, which was used in these experiments, shows relatively weak transduction of the liver (Mathiesen et al., 2020). The significance of these findings is that the addition of the Ple394 promoter into the AAV-PhP.eB capsid seems to restrict gene expression to cortical neurons after IV delivery.

The AAV-PhP.eB capsid is known to cross the blood brain barrier (BBB), which allows it to result in expression of a delivered gene in the CNS after IV delivery (Chan et al., 2017). This vector serotype uses the LY6A receptor within the BBB cells to transcytose across the BBB and into the CNS (Huang et al., 2019). Research has also shown that the addition of cell-specific

promoters into AAV constructs can successfully restrict gene expression to specific brain regions (Chan et al., 2017). The Ple394 promoter would offer a new tool for cortex specific gene expression using an intravenous delivery of the AAV-PhP.eB capsid.

The Ple394 promoter sequence was derived from the Ple17 sequence described by Portales-Casamar and colleagues (Portales-Casamar et al., 2010; Leeuw et al., 2014). The Ple17 sequence showed strong expression in the cortex, but also had some expression in other areas such as the brainstem and cervical spinal cord (Portales-Casamar et al., 2010). The brainstem, cervical spinal cord, and cortex may both use promoter sequences like the Ple17 and Ple394 sequences, which explains the presence of some eGFP positive neurons in these off-target areas of mice that received Ple394 in this study as well (Figure 2). Limitations to this experiment include a lack of quantitative measurements of the numbers of eGFP positive cells per treatment group. Without quantitative measurements, definitive conclusions about the significance of the effect of the addition of the Ple394 promoter on targeted gene expression are not possible. In addition, the neuronal subtype of the transduced neurons in the cortex was not determined since the immunostain simply targeted eGFP without any additional cell-specific antibodies. To address this, an immunostain with antibodies against eGFP and neuronal subtype markers may be warranted, and colocalization of both signals would allow one to determine how many of the eGFP positive neurons are specific subtypes of neurons.

The reason one would desire to reduce expression in non-cortical areas while maintaining strong expression in the cortex would be to add novel sequences, such as the Ple394 sequence, to a database toolbox. This toolbox can serve researchers who want to selectively target gene expression to specific areas, such as the cortex, for their research needs. A possible research use for this vector would be to selectively deliver therapeutics to the cortex for treatment of

Alzheimer's disease, a neurodegenerative disease which affects the cortical regions of the brain (Fjell et al., 2014).

Ple394-HBB:

The Ple394-HBB vector construct resulted in a lack of gene expression of the eGFP reporter gene in the target region, cerebral cortex, after intravenous (IV) injection (Figure 4). The Ple394-HBB vector construct still showed some expression in off-target areas such as the brainstem (Figure 4). The significance of these findings is that the addition of the Ple394-HBB promoter into the AAV-PhP.eB capsid failed to cause restricted gene expression in cortical neurons after IV delivery of the vector.

The Ple394-HBB vector construct is similar to the Ple394 vector construct used in these experiments, with some important changes. The Ple394 promoter sequence was a bit large at 2,232 bp. AAV capsids are known to have restricted genome capacity, about 4.7 kb, to carry gene therapy sequences (Wang et al., 2019). Therefore, it would be useful to reduce the size of the promoter sequence used to target the gene therapy as much as possible, while still retaining strong and specific gene expression targeting in target regions. This would allow for more space to be used by a desired genetic sequence in future gene therapy studies. The human beta-globin (HBB) minimal promoter sequence is 57 bp, which is much smaller than the promoter region of the Ple394 sequence used in the Ple394 vector construct. After replacing the Ple394 promoter sequence with the HBB minimal promoter, while keeping the Ple394 enhancer sequences the vector ended up being 656 bp shorter. Thus, the HBB minimal promoter sequence was used to replace the Ple394 promoter sequence while keeping the Ple394 enhancer regions as shown in Figure 1. The Ple394-HBB construct is smaller than the Ple394 construct, allowing that saved

space to be used for potentially larger gene therapies to be delivered with this vector. The Ple394-HBB promoter would have thus offered an additional new tool for cortex specific gene expression using an intravenous delivery of the AAV-PhP.eB capsid if it had worked.

The Ple394-HBB promoter sequence was also a derivation from the Ple17 sequence described by Portales-Casamar and colleagues (Portales-Casamar et al., 2010; Leeuw et al., 2014). The Ple17 sequence showed strong expression in the cortex, but also had some expression in other areas such as the brainstem (Portales-Casamar et al., 2010). This could explain why there was some eGFP-positive cells in the brainstem of mice treated with the Ple394-HBB. A possible explanation for the gene expression patterns seen in the treated mice is that the core promoter regions that were removed from the Ple394 sequence to insert the HBB minimal promoter sequence were required for the promoter's cortical neuron specificity. Thus, once these sequences were removed, the Ple394 construct failed to cause gene expression in the cerebral cortex. It is worth noting that the results from this experiment suggest that the core promoter sequence is critical for cortex specificity of the Ple394 sequence. Future studies may want to look at replacing the enhancer regions with shorter sequences to shorten the overall size of the promoter sequence while retaining specificity. Limitations to this experiment include a lack of quantitative measurements of the numbers of eGFP positive cells per treatment group. Without quantitative measurements, statistical conclusions about the significance of the effect of the addition of the Ple394-HBB promoter on targeted gene expression are not possible. To address this, cell-counting software could be used to count the number of eGFP positive cells in target areas between positive control and the Ple394-HBB group.

HB9:

The HB9 vector construct resulted in strong expression in cervical spinal motor neurons (Figure 5). The HB9 vector construct also resulted in minimal gene expression of the eGFP reporter gene in the brain (Figure 6). In addition, the HB9 vector at the medium and high doses didn't result in significantly different expression of eGFP in the liver compared to mice that received saline (Figure 7). Meanwhile, the positive control CAG vector resulted in significantly increased expression of eGFP in the liver compared to saline (Figure 7). The significance of these findings is that the addition of the HB9 promoter into the AAV-PhP.eB capsid seems to restrict gene expression to spinal motor neurons after IV delivery.

As mentioned previously, research has shown that the addition of cell-specific promoters into AAV constructs can successfully restrict gene expression to specific brain regions (Chan et al., 2017). The HB9 promoter would offer a new tool for spinal motor neuron specific gene expression using an intravenous delivery of the AAV-PhP.eB capsid. Limitations to this experiment include a lack of quantitative measurements of the ratios of eGFP positive cells that are confirmed to be motor neurons to the total amount eGFP positive cells. Without quantitative measurements, definitive conclusions about the significance of the effect of the addition of the HB9 promoter on targeted gene expression are not possible.

The reason one would desire to specifically target spinal motor neurons would be to add novel sequences, such as the HB9 sequence, to a database toolbox. This toolbox can serve researchers who want to selectively target gene expression to specific areas, such as spinal motor neurons, for their research needs. A possible research use for this vector would be to selectively deliver therapeutics to the spinal motor neurons for treatment of amyotrophic lateral sclerosis (ALS), a neurodegenerative disease which affects the motor neurons of the spinal cord (Rowland, 2001). In addition, future studies should focus on identifying additional promoter

sequences that can also be added to the vector construct to restrict gene expression to other CNS regions, which would further add to the promoter toolbox.

Materials and Methods

Preparation and intravenous delivery of AAV-PhP.eB

The Ple394 vector construct experiments consisted of fourteen mice (seven female and seven male) injected at an age of 11 weeks. Three dosages of this vector were used: $6.25x10^{10}\ vg/\ 150\ \mu L$ (two males and one female), $1.25x10^{11}\ vg/\ 150\mu L$ (four males and five females), $2.50x10^{11}\ vg/\ 150\mu L$ (one male and one female). The mice were all treated with 150μL of intravenous AAV-PhP.eB-Ple394-SI diluted in PBS. The Ple394-HBB vector construct experiments consisted of four mice (two males and two females) injected at an age of 12 weeks. The mice received 150μL ($1.25x10^{11}\ vg/150\mu L$) of intravenous AAV-PhP.eB-Ple394-HBB-SI diluted in PBS. The HB9-HBB vector construct experiments consisted of eighteen mice (eight males and ten females) injected at an age of 10-12 weeks. Three dosages of this vector were used: $6.25x10^{10}\ vg/150\mu L$ (one males and two females), $1.25x10^{11}\ vg/150\mu L$ (four males and four females), $2.50x10^{11}\ vg/150\mu L$ (three males and four females). The mice were all treated with 150μL of intravenous AAV-PhP.eB-HB9-HBB-SI diluted in PBS. The negative control group consisted of nine mice (five males and four females) injected at an age of 10-19 weeks. All mice were injected with 150μL of intravenous PBS. The positive control groups consisted of eight mice (four males and four females) injected at an age of 12 weeks. The mice received 150μL ($1.25x10^{11}\ vg/150\mu L$) of intravenous AAV-PhP.eB-CAG diluted in PBS**.** The mice were sedated using 1% isoflurane/1.5% oxygen and the treatments were injected into the retro-orbital sinus (Gessler et al., 2019). As described by Gessler and colleagues (2019), the needle was inserted at the base of the eye parallel to the rostral/caudal axis of the head. The treatments were delivered at the junction of the ophthalmic veins.

Tissue perfusion and dissection

All mice were sacrificed, perfused with saline, then dissected after a period of four weeks, except for one saline treated mice (n=1) and the AAV-PhP.eB-HB9-HBB treated mice (n=18) which were sacrificed after a period of five weeks. These 19 mice were sacrificed and perfused after a period of five weeks. The liver, lungs, heart, kidneys, gonads, spleen, and diaphragm muscle were dissected from the mice and immediately placed in dry ice before being stored at -80°C. The brains were cut from the spinal cord and removed from the skull. The brains and spinal columns were then drop-fixed for 24 hours in 4% paraformaldehyde in 0.1M phosphate buffer (4% PFA) at 4°C, cryoprotected for a minimum of 72 hours in 30% sucrose at 4°C. The brains were then sectioned sagittally to 40μm thickness and light-level immunohistochemistry was performed against the eGFP protein. The cervical, lumbar, and sacral segments of the mouse spinal cords were dissected from the spinal column and stored at 4°C in 30% sucrose. The cervical dorsal root ganglions (DRG) were also dissected from the mice and also stored at 4°C in 30% sucrose. The cervical and lumbar segments of the spinal cords were sectioned transversely to 40μm thickness and fluorescent immunohistochemistry was performed against the eGFP protein.

Immunohistochemistry and immunofluorescent staining and microscopy

Free-floating sagittal brain sections were first washed in tris-buffered saline (TBS), incubated in methanol, then blocked in 5% donkey serum and 0.25% Triton X-100 in TBS for 1 hour. The tissue was then incubated in rabbit anti-GFP (Invitrogen #A11122) primary antibody diluted to 1:10,000 in blocking solution overnight at 4°C. The following day, sections were washed in TBS and then incubated in Jackson Biotinylated Donkey anti-Rabbit antibody diluted to 1:200 in TBS for 1 hour. Then, the brain sections were incubated in ABC solution, developed

in 3,3′-Diaminobenzidine (DAB) for 7 minutes. The immunostained sections were mounted on gelatin-coated microscope slides and coverslipped using DPX mounting medium.

Free-floating transverse cervical spinal cord sections were first washed in TBS then blocked in 5% donkey serum and 0.25% Triton X-100 in TBS for 1 hour. The tissue was then incubated in Aves GFP-1020 Chicken anti-GFP (diluted to 1:1,000), Genetex GTX82725 Goat anti-ChAT (diluted to 1:200), and Millipore abn90 Guinea Pig anti-NeuN (diluted to 1:1,000). All antibodies were diluted with blocking solution. The tissue was incubated for one overnight at 4°C. The following day, sections were washed in TBS and then incubated in the following secondary antibodies: Donkey anti-Chicken AF488 (diluted to 1:500), Donkey anti-Goat AF555 (diluted to 1:500), Donkey anti-Guinea Pig AF647 (diluted to 1:500), and DAPI (diluted to 1:1,000) for 2 hours in the dark. Then, the tissues were washed in TBS and the immunostained sections were mounted on gelatin-coated microscope slides and coverslipped using Mowiol mounting medium.

Brightfield microscopy was performed on mounted brain and spinal cord tissues using an AxioScan.Z1 Automated Slide Scanner (Zeiss) and 10X Plan Apo objective.

QRT-PCR, analysis, and statistics

Reverse transcriptase quantitative polymerase chain reaction (qRT-PCR) was performed on the livers of mice that received medium dose AAV-PhP.eB-Ple394, medium dose AAV-PhP.eB-HB9-HBB, high dose AAV-PhP.eB-HB9-HBB, positive, or negative control treatments. Each liver was placed in 1mL of Trizol reagent inside a bead ruptor tube and spun on a homogenizer machine at a speed of 4 m/s for 2 cycles of 30 seconds with a 10 second dwell. The homogenized solution was treated with 200 μL of chloroform, inverted, and centrifuged for 15

minutes at 12,000 RPM at 4°C. The supernatant was removed and placed in a new tube then treated with 600μL of 70% ethanol before it was inverted several times. 700μL of that solution was transferred to a QIAGEN RNEasy mini-kit spin column and the protocol was followed to isolate RNA. After the final elution, the concentration of nucleic acid isolated was measured using a Nanodrop spectrophotometer. Then, the isolated nucleic acid solution was diluted to a concentration of 200 ng/μL and treated with Invitrogen DNA-free kit 10X buffer and DNase enzyme then heated for 30 minutes at 37°C. Afterwards, 2.3/μL of the inactivation agent from the DNA-free kit was added to the reaction mixture. The mixture was mixed for 5 minutes at room temperature, centrifuged for 2 minutes at 10,000 RPM, and then the supernatant was removed and transferred to a new tube. The concentration from the supernatant was then measured on the same Nanodrop machine as decsribed previously. cDNA was then made from the isolated mRNA using Invitrogen cDNA syntehsis kit. 5 μL of the 5X iScript Reaction Mix and 1 μL of the Reverse Transcriptase was added to each well of a PCR plate. Then, enough of the isolated RNA was added to the well to have 1,000 ng of RNA. The PCR plate was then spun on a centrifuge and placed in a thermocycler for 5 minutes of priming at 25°C, 20 minutes of reverse transcription at 46°C, and 1 minute of reverse transcriptase inactivation at 95°C. The cDNA was then analyzed using a thermocycler. A housekeeping gene, GAPDH, was used to compare against the presence of eGFP. Each sample was ran in triplicate.

The average of the cycle threshold (Ct) values for each set of triplicates was calculated for the GAPDH samples, eGFP samples, non-reverse transcriptase controls (NRTs), and no template controls (NTCs). If any GAPDH average Ct value above one standard deviation of the average Ct of the NRT and NTC values then the sample was not used in the analysis due to failure to amplify GAPDH. This excluded four samples for failure to amplify GAPDH. In

addition, any samples where the GFP Ct was above or within 1 Ct of the average NRT and NTC Ct value was determined to be not detected since we could not interpret this signal as coming from amplification of the GFP sequence since this amount of signal is present in the absence of cDNA. The difference between the average Ct value of the eGFP sample and the average Ct value of the GADPH sample was calculated for each sample giving the number of cycles greater it took GFP to reach the same level as GAPDH in the PCR. From this, the number of copies of GFP mRNA per 100 copies of GAPDH mRNA was calculated. The average and standard error of the fold change from negative control for each treatment group (CAG positive control, medium dose HB9, high dose HB9, and medium dose Ple394) was calculated. A one-way ANOVA with Tukey's post-hoc test was performed on the data to determine whether there were statistically significant differences in the average number of copies of GFP mRNA per 100 copies of GAPDH mRNA amongst the treatment groups (saline, Ple medium dose, HB9 medium dose, HB9 high dose, and CAG positive control).

References

Arber, S., Han, B., Mendelsohn, M., Smith, M., Jessell, T. M., & Sockanathan, S. (1999). Requirement for the homeobox GENE Hb9 in the consolidation of motor Neuron identity. *Neuron, 23*(4), 659-674. doi:10.1016/s0896-6273(01)80026-x

Brown, R. H., & Al-Chalabi, A. (2017). Amyotrophic lateral sclerosis. *New England Journal of Medicine, 377*(2), 162-172. doi:10.1056/nejmra1603471

Chan, K. Y., Jang, M. J., Yoo, B. B., Greenbaum, A., Ravi, N., Wu, W. L., Sánchez-Guardado, L., Lois, C., Mazmanian, S. K., Deverman, B. E., & Gradinaru, V. (2017). Engineered AAVs for efficient noninvasive gene delivery to the central and peripheral nervous systems. Nature neuroscience, 20(8), 1172–1179. https://doi.org/10.1038/nn.4593

Castle, M. J., Turunen, H. T., Vandenberghe, L. H., & Wolfe, J. H. (2016). Controlling AAV tropism in the nervous system with natural and engineered capsids. In Gene Therapy for Neurological Disorders (pp. 133-149). Humana Press, New York, NY.

Castle, M. J., Baltanás, F. C., Kovacs, I., Nagahara, A. H., Barba, D., & Tuszynski, M. H. (2020). Postmortem Analysis in a Clinical Trial of AAV2-NGF Gene Therapy for Alzheimer's Disease Identifies a Need for Improved Vector Delivery. *Human gene therapy*, *31*(7-8), 415–422. https://doi.org/10.1089/hum.2019.367

Center for Drug Evaluation and Research. (n.d.). Novel Drug Approvals for 2021. Retrieved February 02, 2021, from https://www.fda.gov/drugs/new-drugs-fda-cders-new-molecular-entities-and-new-therapeutic-biological-products/novel-drug-approvals-2021

de Leeuw, C. N., Dyka, F. M., Boye, S. L., Laprise, S., Zhou, M., Chou, A. Y., Borretta, L., McInerny, S. C., Banks, K. G., Portales-Casamar, E., Swanson, M. I., D'Souza, C. A., Boye, S. E., Jones, S. J., Holt, R. A., Goldowitz, D., Hauswirth, W. W., Wasserman, W. W., & Simpson, E. M. (2014). Targeted CNS delivery using human MiniPromoters and demonstrated compatibility with adeno-associated viral vectors. Molecular Therapy. Methods & Clinical Development, 1, 5. https://doi.org/10.1038/mtm.2013.5

Deverman, B. E., Pravdo, P. L., Simpson, B. P., Kumar, S. R., Chan, K. Y., Banerjee, A., Wu, W. L., Yang, B., Huber, N., Pasca, S. P., & Gradinaru, V. (2016). Cre-dependent

selection yields AAV variants for widespread gene transfer to the adult brain. Nature biotechnology, 34(2), 204–209. https://doi.org/10.1038/nbt.3440

Dunbar, C. E., High, K. A., Joung, J. K., Kohn, D. B., Ozawa, K., & Sadelain, M. (2018). Gene therapy comes of age. Science, 359(6372). https://doi.org/10.1126/science.aan4672

Farrer, L. A. (1997). Effects of age, sex, and ethnicity on the association between apolipoprotein e genotype and alzheimer disease. JAMA, 278(16), 1349. doi:10.1001/jama.1997.03550160069041

Fjell, A. M., McEvoy, L., Holland, D., Dale, A. M., & Walhovd, K. B. (2014). What is normal in normal aging? Effects of aging, amyloid and Alzheimer's disease on the cerebral cortex and the hippocampus. *Progress in Neurobiology*, *117*, 20–40. https://doi.org/10.1016/j.pneurobio.2014.02.004

Foust, K. D., & Kaspar, B. K. (2009). Over the barrier and through the Blood: To Cns delivery we go. Cell Cycle, 8(24), 4017-4018. doi:10.4161/cc.8.24.10245

Gao, G., Vandenberghe, L. H., Alvira, M. R., Lu, Y., Calcedo, R., Zhou, X., & Wilson, J. M. (2004). Clades of adeno-associated viruses are widely disseminated in human tissues. Journal of Virology, 78(12), 6381-6388. doi:10.1128/jvi.78.12.6381-6388.2004

Gessler, D. J., Tai, P. W. L., Li, J., & Gao, G. (2019). Intravenous Infusion of AAV for Widespread Gene Delivery to the Nervous System. Methods in Molecular Biology (Clifton, N.J.), 1950, 143–163. https://doi.org/10.1007/978-1-4939-9139-6_8

Hermonat, P. L., & Muzyczka, N. (1984). Use of adeno-associated virus as a mammalian DNA cloning vector: transduction of neomycin resistance into mammalian tissue culture cells. Proceedings of the National Academy of Sciences, 81(20), 6466-6470. Howard, D. B., Powers, K., Wang, Y., & Harvey, B. K. (2008). Tropism and toxicity of adeno-associated viral vector serotypes 1, 2, 5, 6, 7, 8, and 9 in rat neurons and glia in vitro. Virology, 372(1), 24–34. https://doi.org/10.1016/j.virol.2007.10.007

Hordeaux, J., Yuan, Y., Clark, P. M., Wang, Q., Martino, R. A., Sims, J. J., Bell, P., Raymond, A., Stanford, W. L., & Wilson, J. M. (2019). The GPI-Linked Protein LY6A Drives AAV-PHP.B Transport across the Blood-Brain Barrier. Molecular therapy : the journal of the American Society of Gene Therapy, 27(5), 912–921. https://doi.org/10.1016/j.ymthe.2019.02.013

Hippius, H., & Neundörfer, G. (2003). The discovery of Alzheimer's disease. *Dialogues in clinical neuroscience*, *5*(1), 101–108. https://doi.org/10.31887/DCNS.2003.5.1/hhippius

Hrvatin, S., Tzeng, C. P., Nagy, M. A., Stroud, H., Koutsioumpa, C., Wilcox, O. F., Assad, E. G., Green, J., Harvey, C.D., Griffith, E. C., & Greenberg, M. E. (2019). A scalable platform for the development of cell-type-specific viral drivers. ELife, 8. doi:10.7554/elife.48089

Huang, Q., Chan, K. Y., Tobey, I. G., Chan, Y. A., Poterba, T., Boutros, C. L., Balazs, A. B., Daneman, R., Bloom, J. M., Seed, C., & Deverman, B. E. (2019). Delivering genes across the blood-brain barrier: LY6A, a novel cellular receptor for AAV-PHP.B capsids. PloS One, 14(11), e0225206. https://doi.org/10.1371/journal.pone.0225206

Leach, K. M., Vieira, K. F., Kang, S.-H. L., Aslanian, A., Teichmann, M., Roeder, R. G., & Bungert, J. (2003). Characterization of the human β-globin downstream promoter region. Nucleic Acids Research, 31(4), 1292–1301.

Lee, S., Jurata, L. W., Funahashi, J., Ruiz, E. C., & Pfaff, S. L. (2004). Analysis of embryonic motoneuron gene regulation: Derepression of generalactivators function in concert with enhancer factors. *Development, 131*(14), 3295-3306. doi:10.1242/dev.01179

Manfredsson, F. P., Rising, A. C., & Mandel, R. J. (2009). AAV9: a potential blood-brain barrier buster. Molecular Therapy, 17(3), 403-405

Mori, S., Takeuchi, T., Enomoto, Y., Kondo, K., Sato, K., Ono, F., Iwata, N., Sata, T., & Kanda, T. (2006). Biodistribution of a low dose of intravenously administered AAV-2, 10, and 26 11 vectors to cynomolgus monkeys. Japanese journal of infectious diseases, 59(5), 285– 293

Mathiesen, S. N., Lock, J. L., Schoderboeck, L., Abraham, W. C., & Hughes, S. M. (2020). CNS Transduction Benefits of AAV-PHP.eB over AAV9 Are Dependent on Administration Route and Mouse Strain. *Molecular Therapy - Methods & Clinical Development, 19*, 447–458. https://doi.org/10.1016/j.omtm.2020.10.011

Nakano, T., Windrem, M., Zappavigna, V., & Goldman, S. A. (2005). Identification of a conserved 125 base-pair HB9 enhancer that Specifies gene expression to spinal motor neurons. *Developmental Biology, 283*(2), 474-485. doi:10.1016/j.ydbio.2005.04.017

Naso, M. F., Tomkowicz, B., Perry, W. L., & Strohl, W. R. (2017). Adeno-Associated virus (AAV) as a vector for gene therapy. BioDrugs, 31(4), 317-334. doi:10.1007/s40259-017-0234-5

Petrov, D., Mansfield, C., Moussy, A., & Hermine, O. (2017). ALS clinical Trials Review: 20 years of Failure. are we any closer to registering a new treatment? Frontiers in Aging Neuroscience, 9. doi:10.3389/fnagi.2017.00068

Peviani, M., Kurosaki, M., Terao, M., Lidonnici, D., Gensano, F., Battaglia, E., Tortarolo, M., Piva, R., & Bendotti, C. (2012). Lentiviral vectors carrying enhancer elements of Hb9 promoter drive selective transgene expression in mouse spinal cord motor neurons. Journal of Neuroscience Methods, 205(1), 139–147. https://doi.org/10.1016/j.jneumeth.2011.12.024

Portales-Casamar, E., Swanson, D. J., Liu, L., Leeuw, C. N. de, Banks, K. G., Ho Sui, S. J., Fulton, D. L., Ali, J., Amirabbasi, M., Arenillas, D. J., Babyak, N., Black, S. F., Bonaguro, R. J., Brauer, E., Candido, T. R., Castellarin, M., Chen, J., Chen, Y., Cheng, J. C. Y., … Simpson, E. M. (2010). A regulatory toolbox of MiniPromoters to drive selective expression in the brain. Proceedings of the National Academy of Sciences, 107(38), 16589. https://doi.org/10.1073/pnas.1009158107

Ravindra Kumar, S., Miles, T. F., Chen, X., Brown, D., Dobreva, T., Huang, Q., Ding, X., Luo, Y., Einarsson, P. H., Greenbaum, A., Jang, M. J., Deverman, B. E., & Gradinaru, V. (2020). Multiplexed Cre-dependent selection yields systemic AAVs for targeting distinct brain cell types. *Nature Methods*, *17*(5), 541–550. https://doi.org/10.1038/s41592-020-0799-7

Rosenberg, J. B., Kaplitt, M. G., De, B. P., Chen, A., Flagiello, T., Salami, C., Pey, E., Zhao, L., Ricart Arbona, R. J., Monette, S., Dyke, J. P., Ballon, D. J., Kaminsky, S. M., Sondhi, D., Petsko, G. A., Paul, S. M., & Crystal, R. G. (2018). AAVrh.10-Mediated APOE2 Central Nervous System Gene Therapy for APOE4-Associated Alzheimer's Disease. Human gene therapy. Clinical development, 29(1), 24–47. https://doi.org/10.1089/humc.2017.231

Rowland, L. P. (2001). How amyotrophic lateral sclerosis got its name. *Archives of Neurology*, *58*(3). doi:10.1001/archneur.58.3.512

Schultz, B. R., & Chamberlain, J. S. (2008). Recombinant adeno-associated virus transduction and integration. Molecular Therapy, 16(7), 1189-1199.

Shaul, O. (2017). How introns enhance gene expression. *The International Journal of Biochemistry & Cell Biology*, *91*, 145–155. https://doi.org/10.1016/j.biocel.2017.06.016

Verghese, P. B., Castellano, J. M., Garai, K., Wang, Y., Jiang, H., Shah, A., Bu, G., Frieden, C., & Holtzman, D. M. (2013). Apoe influences amyloid- (a) clearance despite minimal apoe/a association in physiological conditions. Proceedings of the National Academy of Sciences, 110(19). doi:10.1073/pnas.1220484110

Wang, D., Tai, P. W. L., & Gao, G. (2019). Adeno-associated virus vector as a platform for gene therapy delivery. Nature Reviews. Drug Discovery, 18(5), 358–378. https://doi.org/10.1038/s41573-019-0012-9

Yiannopoulou, K. G., & Papageorgiou, S. G. (2012). Current and future treatments for alzheimer's disease. Therapeutic Advances in Neurological Disorders, 6(1), 19-33. doi:10.1177/1756285612461679

Zhao, L., Gottesdiener, A. J., Parmar, M., Li, M., Kaminsky, S. M., Chiuchiolo, M. J., Sondhi, D., Sullivan, P. M., Holtzman, D. M., Crystal, R. G., & Paul, S. M. (2016). Intracerebral adeno-associated virus gene delivery of apolipoprotein E2 markedly reduces brain amyloid pathology in Alzheimer's disease mouse models. Neurobiology of aging, 44, 159–172. https://doi.org/10.1016/j.neurobiolaging.2016.04.020